Supporting Online Material for

Niche and neutral effects of acquired immunity permit coexistence of pneumococcal serotypes

Sarah Cobey and Marc Lipsitch

correspondence to: scobey@hsph.harvard.edu

This PDF file includes:

Materials and Methods

S1 Analysis of carriage studies

To quantify pneumococcal diversity in natural carriage, we analyzed nasopharyngeal carriage studies selected by the following criteria: isolates had to be collected over ≤1 y, sampled individuals were not chosen because of suspected or confirmed pneumococcal disease or a predisposing condition (e.g., sick cell anemia or HIV), the conjugate vaccine could not be in use in the population, the most common isolates had to be serotyped (i.e., resolved past the serogroup level), the serotypes of at least half of the typed isolates had to be reported (studies in which it was not clear that the most frequent serotypes were listed were excluded), and ≥50 isolates had to be typed and reported. Nontypable isolates were excluded from totals. When a study included distributions for multiple locations or age groups, we included the subset of data with the smallest spatial and age resolutions meeting the criteria. If a study gave data from multiple point prevalence estimates within a 2-y span, we included data from one of the sampling times. The studies varied widely in whether they reported the serotypes or serogroups of the less common types (e.g., 12, 16, 22, and 10). To retain statistical power, we allowed inconsistencies, though we required that included studies differentiate the serotypes of the most common serogroups (6, 19, and 23). We combined counts of 15B and 15C into a single 15B/C category because these types mutate easily into the other type (*33, 34*).

The studies were loosely grouped by the age range of sampled hosts. The majority of carriage studies involve young children less than 6 y old (Table S1). Only two studies meeting our criteria reported serotype frequencies for older children and adults. Two studies reported carriage frequencies from a random sample of the population, and two reported aggregated frequencies from children and their close adult contacts.

To calculate the Simpson Index (*35*), we pared the data sets to those in which the typed isolates were identified to the serotype level (i.e., <3% of isolates were marked as "other" or as a list of serotypes; Table S1). The mean Simpson Index was 0.90 (range 0.86-0.94, $n = 2$) in infants; 0.90 (range 0.88-0.94, $n = 8$) in young children; 0.94 in older children and adults (range 0.93-0.96, $n = 2$); and 0.94 in a random sample of a population. The mean Simpson Index of these studies after removing duplicates (i.e., considering only the whole-population and not age-specific distributions from (*20*)) was 0.91 ± 0.03 S.D. ($n = 11$). We determined by Pearson's linear correlation that there was no significant relationship between age-specific prevalence and the Simpson Index in studies of infants and young children ($\rho = 0.45$, $p = 0.20$, $n = 10$).

We generated rank-frequency distributions for each study by calculating the fraction of isolates comprised by each serotype out of all typed isolates (Fig. S1). We found no significant relationship between age-specific prevalence and the frequency of the commonest type in the two younger age groups. These distributions were then used to calculate means for different age groups (Fig. S2). The distributions of the two youngest age groups are very similar, with the commonest type in both groups having a mean frequency of 0.18. The distribution of the older age groups appears more even (flatter), though due to the small sample sizes, any differences cannot be distinguished statistically. We calculated the mean of all studies (again using only the whole-population curve from (*20*)) and plotted it alongside the two distributions from randomly sampled populations. The curve from (*12*) appears significantly more even than the mean of the

aggregated studies. This study may be an ecological outlier: it analyzed a population with an extremely high carriage prevalence (97% in young children and 72% overall).

We also analyzed the consistency of serotypes' rankings. First, we considered those studies in infants and young children in which at least ten serotypes were reported, and we calculated the average number of serotypes shared among the ten most frequent serotypes between all study pairs. Due to differences in the typing of serogroup 15, we considered any shared serotypes within this group a match. (No studies included two serotypes of serogroup 15 in the top 10 types.) The average number of shared serotypes in the top ten was 6.9 ± 1.0 S.D. (n = 14 studies). Second, we observed the breadth in serotypes' rankings (Fig. S3) in the same set of studies and found that certain serotypes—namely, 6A, 6B, 19F, and 23F—were both highly ranked and consistently present. Serotypes' ranks generally appeared clustered (i.e., not random) though variable. Serotype 14, for example, was the second most frequent type in one study and the ninth most frequent type in two.

S2 Epidemiological model

S2.1 The force of colonization

At discrete time steps, the force of colonization on a host for each serotype z in the simplest (and default) model was computed following

$$\lambda(z) = q(z,\vec{\theta},\vec{C})\left[\beta\frac{I_z}{N} + w\right]. \quad \text{(S1)}$$

The term $q(z,\boldsymbol{\theta},\mathbf{C})$ is the host's susceptibility, or probability of acquiring serotype z, contingent on the vectors of past colonizations $\boldsymbol{\theta}$ and current carriage $\mathbf{C}$. Vectors $\boldsymbol{\theta}$ and $\mathbf{C}$ are both indexed by serotype. Entries of $\boldsymbol{\theta}$ count the number of times the host has cleared each serotype, and $\mathbf{C}$ counts the number of current colonizations with each serotype. The contact rate, β, is shared by all serotypes. The effective fraction of hosts colonized with serotype z, I_z/N, equals the number of colonizations with z in the population divided by the population size N. This representation means that hosts who are colonized with a single strain of serotype z are counted once, and hosts harboring more than one strain of serotype z are counted multiple times; this formulation avoids biasing the model toward coexistence (*14*). A constant, very low rate of immigration w of each serotype allows reseeding after stochastic extinctions (e.g., due to oscillations in prevalence) but is set low enough to avoid distorting general patterns in the rank-frequency distributions.

In the model that includes age-assortative mixing, the force of colonization with serotype z on a host of age a is computed by

$$\lambda(a,z) = q(z,\vec{\theta},\vec{C})\left[\sum_{j=1}^{A}\alpha_{aj}\beta\frac{I_{z,j}}{N_j} + w\right]. \quad \text{(S2)}$$

Here, α_{aj} weights contacts by individuals of age j to individuals of age a. The matrix $\boldsymbol{\alpha}$ of these weights was obtained by dividing observed per-capita (i.e., per-j) physical contact rates by individuals of age j with individuals of age a by the population of individuals of age a to obtain an approximation of α_{aj} (*36*). Parameter A denotes the maximum possible host age.

In the model in which host contacts are structured by household, fraction ρ of the force of infection comes from the host's household h (even if the host is its only member), and fraction $(1 - \rho)$ comes from the host's contacts with non-household members. The force of colonization with serotype z for a host in household h is thus given by

$$\lambda(h,z) = q(z,\vec{\theta},\vec{C})\left[\rho\beta\frac{I_z^h}{N^h} + (1-\rho)\beta\frac{\sum_{g\neq h} I_z^g}{\sum_{g\neq h} N^g} + w\right], \tag{S3}$$

where N^h (N^g) denotes the total number of household (non-household) members and I_z^h (I_z^g) the number of strains of serotype z inside (outside) the household.

S2.2 Susceptibility

The host's susceptibility to a serotype is reduced if the host is currently colonized with pneumococcus and further reduced if the host has previously carried (i.e., cleared) that serotype. Assuming $\tau(z) = 0$ if $\boldsymbol{\theta}_z = 0$ (i.e., the host has not previously cleared serotype z) and $\tau(z) = 1$ otherwise, the susceptibility $q(z,\boldsymbol{\theta},\boldsymbol{C})$ is given by

$$q(z,\vec{\theta},\vec{C}) = \omega(\vec{C})\left[1 - \min(1,\sigma\cdot\tau(z))\right], \tag{S4}$$

where $\omega(\mathbf{C}) = 0$ if $\Sigma\mathbf{C}_i = 0$ (i.e., if the host is not carrying pneumococcus). If $\Sigma\mathbf{C}_i > 0$, $\omega(\mathbf{C})$ gives the reduction in susceptibility to an invading serotype caused by immediate exclusion by the most fit resident. If $\boldsymbol{f}$ is the vector of fitness ranks of the carried serotypes (ranked against all serotypes), with $\min(\boldsymbol{f})$ denoting the most fit carried serotype, the reduction in susceptibility is given by

$$\omega(\vec{C}) = \mu_{\max}\left[1 - \frac{\min(\vec{f}) - 1}{Z - 1}\right]. \tag{S5}$$

The total number of pneumococcal serotypes is given by Z. Function S5 scales the resistance to acquisition of a new serotype, such that the most fit serotype reduces acquisition by a fraction $\mu_{\max}$, and this resistance declines to zero for the least fit serotype.

Complete or perfect anticapsular immunity corresponds to $\sigma = 1$ and no anticapsular immunity to $\sigma = 0$. Susceptibility to a pneumococcal serotype is thus reduced by a constant fraction σ if the host has previously cleared that serotype.

S2.3 Duration of carriage

When a host becomes colonized with a strain of serotype z, a duration of carriage for that colonization event is drawn from an exponential distribution with mean $\nu(z)$. The mean depends on the serotype-specific duration of carriage in the absence of immunity, $\gamma(z)$, and the total number of past colonization events, independent of serotype:

$$\nu(z) = \kappa + \left[\gamma(z) - \kappa\right]\exp\left(-\varepsilon\sum_i \theta_i\right). \tag{S6}$$

The minimum duration of carriage, which is constant across serotypes, is given by κ. The exponential is a parsimonious approximation of the durations of carriage observed in a prospective study of children tracked from birth (Fig. S4)(*17*). Two linear models were also tested. These models had the form

$$\nu(z) = \max\left(0, \gamma(z) - \varepsilon_{\text{lin}} \sum_i \theta_i\right). \quad \text{(S7)}$$

The models are distinguished throughout the manuscript by their use of ε or ε_{lin} to set the rate of acquisition of nonspecific immunity. Higher values of ε and ε_{lin} correspond to a faster acquisition of nonspecific immunity, though they might also partially reflect a maturation of the immune system with age (*37*). The values used are described in Section S4.

S2.4 Vaccination

When modeled, the vaccine was assumed to have a specific efficacy p for all targeted serotypes and became effective in all hosts at age a_{v} starting in year 400. Vaccine-induced immunity functioned analogously to naturally acquired anticapsular immunity, and susceptibility to a serotype following vaccination was

$$q(z, \vec{\theta}, \vec{C}) = \omega(\vec{C}) \min\left[(1-p), 1 - \min(1, \sigma \cdot \tau(z))\right]. \quad \text{(S8)}$$

S3 Demographic model

Aside from the straightforward birth, aging, and death processes, most of the details of the demographic simulation are relevant only to the few models tested that contain population structure (i.e., use equations S2 or S3 to calculate the force of infection).

The demographic component of the simulation was event-driven. The possible demographic events were births, deaths, departures from the household of origin, partnering, and reproduction. At birth, ages were stochastically assigned for each of an individual's major life events using stationary distributions of the age at death, the age of leaving home, the age at partnering (though not all hosts partner), and the age(s) at which children, if any, are born (Fig. S5).

The probability mass function for the total number of offspring (parity) was computed assuming observed densities of lifespans and maternal ages at birth while requiring the population size to remain constant. The parity distribution was adjusted to encourage large households with children. No minimum interval was imposed on the time between births, and birth rates were independent of partnering status and whether the individual had left her household of origin. Except for the net zero growth rate, these distributions were chosen to reflect demographic dynamics in an industrialized country in the late 20$^{\text{th}}$ century.

At birth, an age of initiating a partnership was drawn for a certain fraction of individuals from a probability mass function. The function was drawn from a truncated negative binomial distribution assuming a median age of 22 y and a minimum age of 16 y. At this age, the initiator leaves its household of origin if it has not already done so and creates a new household. The individual then randomly chooses an unpaired individual within a particular age range. The chosen partner joins the initiator's household. If the chosen partner was living independently with children, these children also join the

initiator's household. For computational convenience, we assumed that if the chosen partner was living in its household of origin, any children are left behind; partnerships can only be disrupted by death; widowed individuals cannot remarry; and any orphaned children remain orphaned.

At birth, all individuals were assigned a date at which they would leave their household of origin. As described, this event could be preempted by partnering, which required that partners move from their households of origin.

S4 Parametrization

Table S2 shows the parameters used in the different versions of the model.

S4.1 Comments on the epidemiological parametrization

For every combination of parameters, the transmission rate (β) was fit to obtain a specific total prevalence of pneumococcal carriage (default, 40%) in children <5 y old. To fit the transmission rates, the average carriage prevalence in children was calculated from annual strobes in the final 10 y of the simulation. A mean prevalence within 1% of the target prevalence (e.g., 39%-41% for a target prevalence of 40%) was considered acceptable.

The rate of acquisition of nonspecific immunity was determined by fitting ε by nonlinear least squares to the mean observed durations of individual serotypes in (*17*), assuming a minimum carriage duration of 25 days (*8*) and the functional form described by equation S6. Point estimates of ε ranged from 0.15 (for serotype 14) to 0.36 (for serotype 23). They had a mean of 0.25, which was used as the default. (This value was also close to the estimated ε for "other types.") The mean observed durations were also fit by nonlinear least squares to the linear model (equation S7), yielding $\varepsilon_{\text{lin}} = 25$. Because the durations in (*17*) reflect only the first few colonizations and contain no information about the tail of the distribution (which for the exponential model was supplied by observations in (*8*)), $\varepsilon_{\text{lin}} = 12.5$ was also included.

For simplicity, we chose to distribute the serotypes' intrinsic durations of carriage—a proxy for fitness—evenly over the interval [25, 220] days. Two studies (*12, 17*) ("Gray" and "Hill" in Fig. S6) have examined durations of carriage as a function of the number of times a host has acquired pneumococcus; the primary colonizations reveal the intrinsic duration of a handful of serotypes and serogroups. Several studies (e.g., (*8*)) have estimated durations of serogroups as a function of host age. Because children typically have multiple carriage episodes in their first year of life, these age-based estimates should underestimate the intrinsic durations of carriage. The estimates have been included for comparison.

To simulate the heptavalent conjugate vaccine (PCV7), the simulated targeted serotypes were chosen to have the same rankings as the actual targeted serotypes. Because of ambiguity in actual rankings, several different sets were used. The details are described in Section S7.1.

S4.2 Comments on the demographic parametrization

The mean number of offspring was calculated numerically assuming a constant population size, and the skew of the distribution of the lifetime number of children was manually adjusted to approach that of the United States. Larger numbers of offspring

among reproducing females were favored to increase the probability of detecting an effect of households on diversity.

S5 Simulation methods

Every model (unique set of parameter values) was simulated ten times. Simulations were run for 300 y to allow the demographic dynamics to equilibrate before the populations were seeded with pneumococcal serotypes. The combined epidemiological and demographic dynamics were simulated for another 150 y. The force of colonization of each host was calculated daily, and any predicted colonization events were randomly scheduled to occur before the next time step. All other events were scheduled exactly.

Additional results

S6 Dynamics of the base model

Except where indicated, the simulations do not include population structure (i.e., age-assortative or household-dependent mixing) or vaccination.

S6.1 Sample trajectories

Figure S7 compares the simulated and observed household and age distributions. Figure S8 shows sample demographic and epidemiological dynamics from one simulation using the default parameters. To confirm that 150 y of simulated epidemiology (i.e., years 300-450 of the total simulation) accurately represent long-term dynamics, we ran the epidemiological dynamics for 500 y. Judging by eye, we saw no new patterns in the extended simulation (results not shown).

S6.2 Rank frequency and correlations

In addition to the Simpson Index, we examined the distributions of rank frequencies and the stability of serotype rankings across simulations for different values of anticapsular immunity σ and rates of acquiring nonspecific immunity (ε and ε_{lin}). For every tested value of ε, simulated rank frequencies could fall within the observed distribution for some nonzero amount of anticapsular immunity (Fig. S9). For example, when $\varepsilon = 0.1$, a realistic distribution appeared at $\sigma = 0.6$. At higher values of ε ($\varepsilon = 0.25$ and $\varepsilon = 0.4$), realistic distributions were possible at $\sigma = 0.3$. In contrast, when acquired nonspecific immunity was associated with a linear decline in serotypes' durations of carriage ($\varepsilon_{lin} = 12.5$ and $\varepsilon_{lin} = 25$), the observed pattern of rank frequency could not be reproduced for any amount of anticapsular immunity.

The average number of top-ranking serotypes shared between replicate simulations measures the stability of the rank order. When the duration of carriage decays exponentially with past exposure, the stability of the rank order is relatively insensitive to the strength of anticapsular immunity (Fig. S10). Both $\varepsilon = 0.25$ and $\varepsilon = 0.4$ produce rank orders consistent with observations. When nonspecific immunity is acquired more slowly ($\varepsilon = 0.1$), intermediate levels of anticapsular immunity ($\sigma = 0.2$-0.6) are associated with a significantly less variable rank order. A strongly preserved rank order is also characteristic of the models with a linear decline in the duration of carriage ($\varepsilon_{lin} = 12.5$ and $\varepsilon_{lin} = 25$) at high levels of anticapsular immunity (e.g., $\sigma = 0.8$). Inspection of sample simulations reveals that much of the variability in order at lower levels of anticapsular

immunity arises from stochastic fluctuations of extremely rare types, and at higher levels, it arises from longer-term fluctuations in the prevalence of endemic serotypes.

S6.3 Duration of carriage and age

As an additional test of the models, we calculated the expected durations of carriage as a function of host age, since this (rather than duration as a function of exposure) is usually measured in population-based studies. The durations were calculated using equations S6 and S7 and hosts' vectors of past carriage at the final time step. We grouped hosts into one-year cohorts and show the expected duration of serotype 0 (the serotype with the highest intrinsic fitness) (Fig. S11). The observed shapes are most consistent with the faster exponential decline in the duration of carriage with exposure (i.e., a fast acquisition of nonspecific immunity; $\varepsilon = 0.25$ and $\varepsilon = 0.4$) with some anticapsular immunity ($\sigma = 0.3$, 0.6, or 0.9). Linear declines in carriage duration with exposure generally do not produce a realistic shortening of duration with age except potentially at $\varepsilon_{lin} = 25$ and $\sigma = 0.9$.

S6.4 Serotype diversity and age

Using the Simpson Index, we examined the diversity of colonizing serotypes as a function of the strength of anticapsular immunity and host age (Fig. S12). In the models in which the durations of carriage decayed exponentially with exposure ($\varepsilon = 0.1$, 0.25, or 0.4) and in which anticapsular immunity was present ($\sigma = 0.3$, 0.6, or 0.9), diversity was significantly higher in older age groups (5-20 y and >20 y) than in younger age groups (<1 y and 1-2 y). The differences were modest and on par with observations (Section S1 and (*25*)). In contrast, when the durations of carriage were linearly correlated with exposure, diversity in hosts >5 y old was actually lower than in younger age groups. Because older hosts tended to have had acquired substantial nonspecific immunity, they were unable to carry all but the fittest serotypes. With $\varepsilon_{lin} = 25$, individuals >20 y old had accumulated so much nonspecific immunity that they were generally incapable of carrying pneumococcus (i.e., they cleared colonizing serotypes almost immediately).

S6.5 Co-colonizations

Observational studies have estimated that 10% (*38*), 11% (*39*), 13% (*40*), and 30% (*41*) of children colonized with pneumococcus carry multiple serotypes (are "co-colonized"). In the models that assumed an exponential decline in carriage duration with exposure, the simulations produced rates of co-colonization were broadly consistent with observations for $\sigma = 0.3$, 0.6, and 0.9 (Fig. S13). In general, the co-colonization rate was higher as anticapsular immunity increased. The models that assumed a linear decline in the duration of carriage produced realistic rates of co-colonization with $\sigma \geq 0.2$; however, at $\varepsilon_{lin} = 25$ and $\sigma = 0.8$ and 0.9, rates were excessively high.

S6.6 Epidemics of rarer serotypes

One of the few long-term data sets of pneumococcus before the introduction of conjugate vaccines observed 5- to 10-y periods of elevated frequencies of individual subdominant (i.e., relatively rare) serotypes (*22*). The changes in frequency were measured through cases of invasive disease, which might not reflect changes in carriage. A consistent finding in models involving some degree of anticapsular immunity were

multi-year elevations in the prevalence of the rarer types. Increasing the amount of anticapsular immunity generally increased the amplitude of these epidemics.

To quantify this pattern, the relative outbreak sizes of the different serotypes were measured by calculating for the last 20 y of every simulation the difference between the current prevalence and its 20-y mean and dividing this quantity by 20-y mean (Fig. S14). Large positive fluctuations, i.e., epidemics, were more common in the rarer serotypes. These fluctuations were further quantified as the mean of the absolute value of these normalized prevalence differences, or the mean prevalence anomaly. For every level of anticapsular immunity, rarer serotypes showed more epidemic-like behavior (Fig. S15). When the prevalence of the rarer serotypes was very low, positive values of the mean prevalence anomaly reflect the role of demographic stochasticity in very small outbreaks. The fact that the size of the deviation increases with the prevalence of these serotypes (i.e., with σ) indicates that relatively large outbreaks by rarer serotypes are a general feature of the dynamics when anticapsular immunity is present.

S6.7 Sensitivity to the number of serotypes

The density or similarity of serotypes' intrinsic fitnesses affected levels of simulated diversity (Fig. S16). Assuming a fixed minimum and maximum intrinsic duration of carriage (25 days and 220 days, respectively), the number of serotypes Z distributed evenly in this range was varied from the default of $Z = 25$ to $Z = 15$ and $Z = 35$. As discussed in the main text, reducing the intrinsic fitness differences between serotypes allowed a greater number to coexist and appeared to change the underlying niche width. Increasing from 25 to 35 serotypes allowed realistic levels of diversity to be simulated starting at $\sigma = 0.2$ rather than $\sigma = 0.3$. The corresponding threshold with 15 serotypes was $\sigma = 0.5$.

S6.8 Sensitivity to the host population size

The diversity predicted by the default model was insensitive to the size of the host population for the values tested (Fig. S16).

S6.9 Sensitivity to the total prevalence

The dynamics of the default model were sensitive to the target carriage prevalence when anticapsular immunity was weak (e.g., $\sigma = 0$ and 0.1; Fig. S16). At these values, a higher carriage prevalence was associated with higher diversity and a lower carriage prevalence with lower diversity. At 60% prevalence in the absence of anticapsular immunity, the second most fit serotype had a relative frequency of approximately 27% instead of 3%. However, increasing the target prevalence from 40% to 60% did not change the level of anticapsular immunity required to match observed diversity.

S6.10 Sensitivity to population structure

We investigated the extent to which simple assumptions about population structure, such as the presence of age-assortative mixing or higher mixing within households, might affect pneumococcal diversity. In our experiments, the presence of population structure had no effect or lowered diversity (Fig. S16). We propose that greater-than-random rates of contact among children might intensify competition among serotypes.

S6.11 Sensitivity to immigration

The effect of immigration should be most pronounced on the low-frequency serotypes. The default immigration rate is equivalent to, for each serotype, one individual in the population being exposed every 20 days to another individual (from outside the population) carrying that serotype. Given a <100% probability that this exposure will result in colonization and durations of carriage of <100 days for these low-ranking serotypes, the immigration itself could only be responsible for fewer than 5 (=100/20) individuals colonized at any given time. The lowest-ranking serotype in the observed distribution has a frequency of 0.0105 ± 0.005, which would be equivalent to ~75-82 individuals colonized with that type (assuming a reasonable 15% total carriage prevalence in the population). This implies that the default immigration rate cannot substantially distort simulated frequency distributions in the area of interest (frequencies $\geq 10^{-2}$), or, put another way, that the low-frequency serotypes have a standing prevalence that reflects mainly endemic transmission, and not the immigration itself.

Consistent with this reasoning, the basic results were unaffected by the small amount of of immigration assumed in the model (Fig. S16). A ten-fold higher rate of immigration predictably increased diversity, but a ten-fold lower rate yielded slightly reduced diversity only at low ($\sigma = 0$, 0.1, and 0.2) and high ($\sigma = 0.9$) levels of anticapsular immunity. At higher values of anticapsular immunity, immigration played a critical role in reseeding populations of low-frequency serotypes after epidemics.

S7 Dynamics of the model with vaccination

S7.1 Changes in diversity and carriage in different vaccination scenarios

Two types of vaccine scenarios were simulated: scenarios in which the T most fit serotypes were targeted by the vaccine (e.g., Fig. 3A and 3F in the main text show $T = 7$ for two different levels of anticapsular immunity, σ), and scenarios in which the targeted serotypes had ranks analogous to the ones included in the real vaccine (e.g., Fig. 3B). Because there is ambiguity in rankings of real serotypes, several different sets of targeted ranks were modeled (Table S3).

Examination of the simulated time series revealed that in children, serotype diversity, as measured by the Simpson Index, generally increased immediately following vaccination when anticapsular immunity was relatively weak and when several of the most fit serotypes were targeted ($0.2 \leq \sigma \leq 0.5$; $T = 7$, $T = 13$, and scenario C in Fig. S17; scenario E in Fig. 3B).

We do not expect diversity in adults necessarily to follow the patterns in children immediately after vaccination. Differences should depend on the amount of anticapsular immunity and the identities of the replacing serotypes.

Targeting enough high-ranking serotypes led to a long-term reduction in carriage prevalence when anticapsular immunity was weaker than vaccine-induced immunity (Fig. S18).

We tested several of the models' assumptions to determine if they might affect the long-term reduction in carriage observed in most simulations. Increasing the age of vaccination from 6 to 12 months in scenario A did not affect long-term changes in carriage prevalence (results not shown). We considered the possibility that serotypes within the same serogroup have identical fitnesses, but their frequencies in carriage differ because naturally acquired anticapsular immunity to one serotype (e.g., 6B, 19F, 23F)

confers some protection to other serotypes in the same serogroup (e.g., 6C, 19A, and 23A respectively). Furthermore, this cross-protection might not be present in vaccine-acquired immunity (*24, 26, 42*). To model this possibility, we assumed that the heptavalent vaccine was effectively pentavalent and did not target serotypes with ranks corresponding to 19F and 23F (because they were interchangeable with 19A and 23A and would be replaced by them). Replacing the heptavalent vaccine in scenario E with this pentavalent version (i.e., the heptavalent with 19F and 23F removed) attenuated the long-term change in carriage prevalence so that it was 4.8 ± 2.2% lower than before vaccination at $\sigma = 0.3$. If serotype 6B was also removed from the simulated vaccine, there was no long-term change in total carriage rates. We suggest that cross-reactive serotype-specific immune responses, which our default model does not include, be investigated as a possible factor to explain potential discrepancies between the real and simulated vaccine's effect on total carriage.

S7.2 Observed changes following vaccination in human populations

The first country with widespread adoption of PCV7 was the United States, which introduced the vaccine in 2000 and had achieved 41% coverage (≥3 doses of the vaccine in children age 19-35 mos.) by 2002, 73% by 2004, and 93% by 2008 (http://www.cdc.gov/vaccines/stats-surv/nis/default.htm#nis). Carriage studies of young children in Massachusetts reported serotype replacement by 2004, accompanied by an increase in diversity that had disappeared by 2007 (*24*). Total carriage prevalence of children declined from 27% in 2001 to 23% in 2004 and then increased to 30% in 2007 (*43*).

England introduced PCV7 in September 2006. In the winter of 2008-2009, the total carriage prevalence in families was 31.9% (v. 24.4% in 2001-2002), a significant increase, though the change was not significant for any individual age group (*25*). At this time, serotype diversity was higher than in 2001-2002. Norway, which introduced PCV7 in July 2006, reported a virtually unchanged carriage prevalence of approximately 80% in children in day-care centers between the fall of 2006 and the fall of 2008, when 38% of children had received ≥2 doses of the vaccine (*40*).

In contrast to the United States, Norway, and England, the Netherlands and France experienced a significant drop in total carriage several years after the introduction of the vaccine. In the Netherlands, which had extremely high and rapid vaccine uptake, there was a 25-30% decline in total carriage in young children (11 mos. and 24 mos.) three years after the introduction of the vaccine (*44*). No change was observed in adults. In France, the prevalence of pneumococcus in children suffering from acute otitis media decreased from 71% to 62%, a significant decline, while the proportion who had received ≥1 dose of PCV increased from 8% to 92% over the same five-year period (*45*).

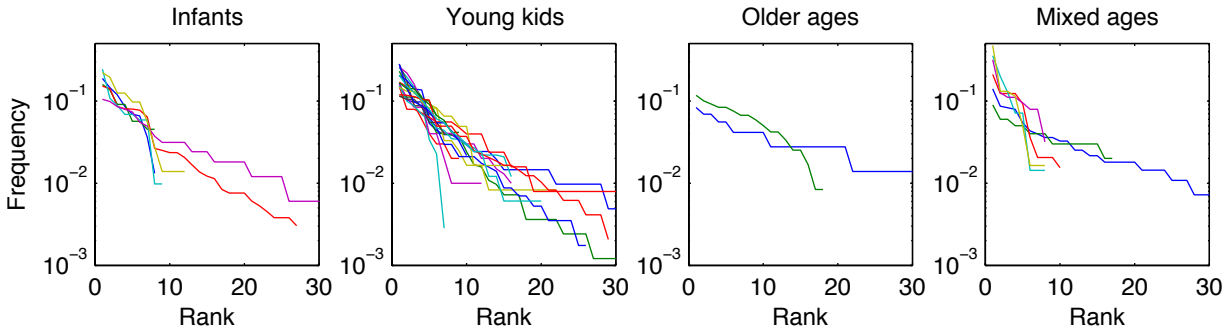

Fig. S1

Rank-frequency distributions from carriage studies. The differently colored curves correspond to individual studies listed in Table S1, and studies are grouped into subplots according to their categories in Table S1.

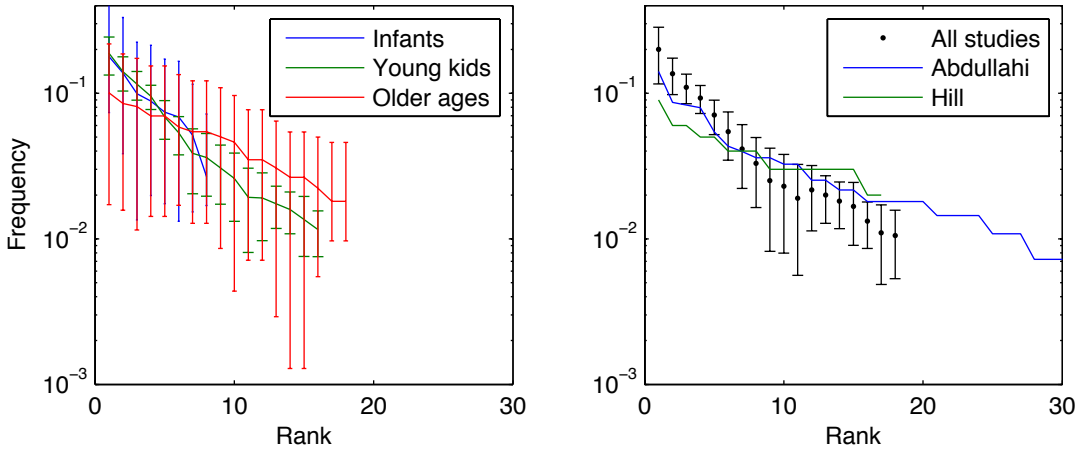

Fig. S2

Left, Rank-frequency distributions obtained from averaging the curves in Fig. S1. Error bars show ranges for infants and older ages and standard deviations for young children. The curves for young children extend to the last rank with ten or more studies; the other curves end when the first study reaches its maximum rank. **Right**, The average rank-frequency distribution of all studies. Error bars denote standard deviations. The blue and green curves show the distributions of the two studies that sampled people randomly.

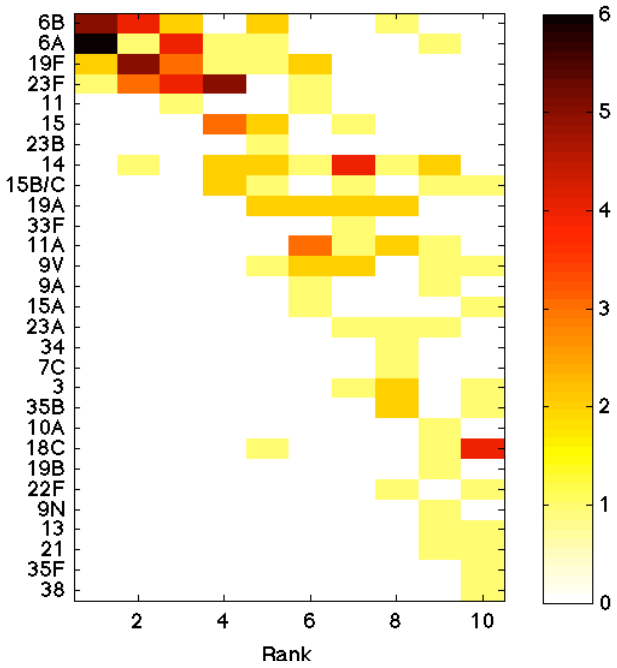

Fig. S3

A histogram of the rankings of serotypes counted among the 10 commonest types in at least one of 14 studies of infants and young children. The color indicates the number of studies in which each rank was observed. Several studies listed only serogroup 15, whereas others mentioned a specific serotype (15A or 15B/C). These variants are listed separately.

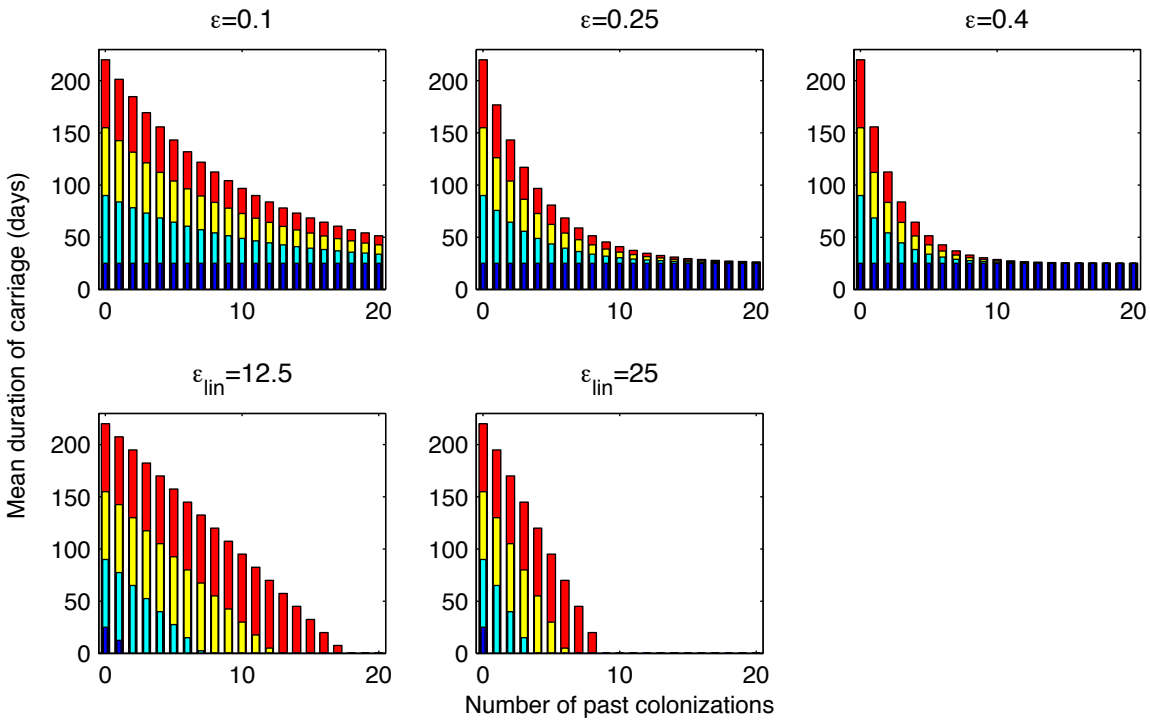

Fig. S4

Mean durations of carriage for four representative serotypes under different assumptions about the rate of acquiring nonspecific immunity. Colors indicate the serotypes' fitnesses, with red (dark blue) denoting the most (least) fit serotypes. Bars are superimposed, not stacked.

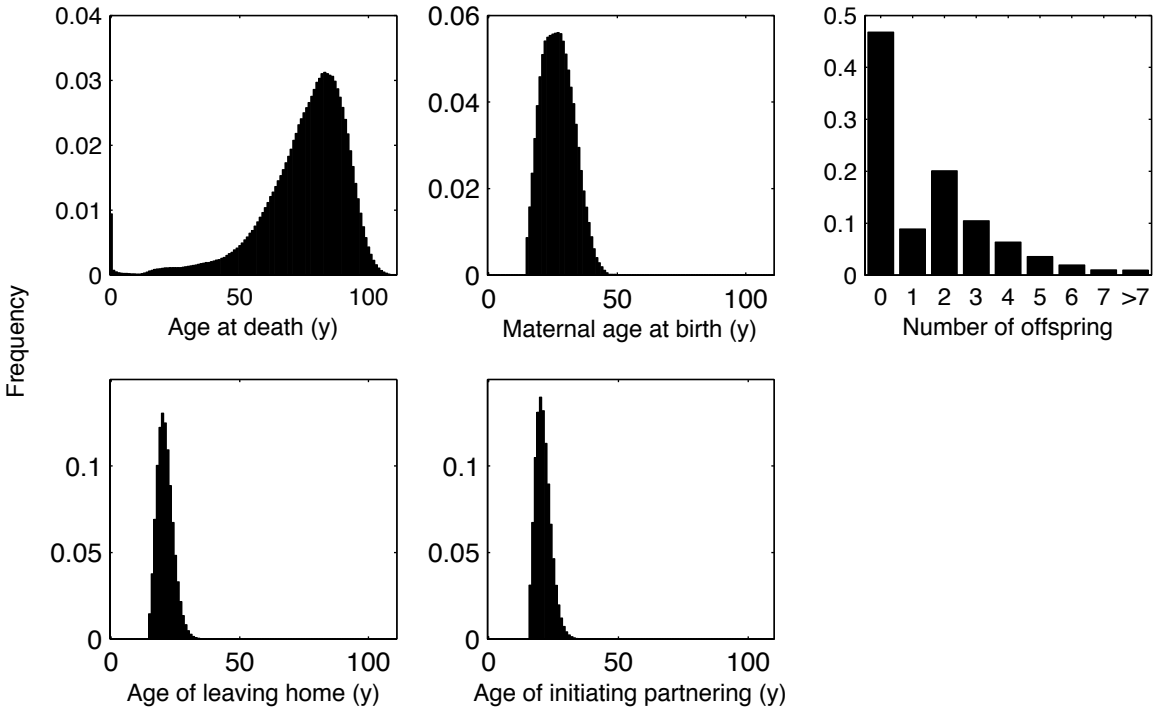

Fig. S5

Probability mass functions used to generate life histories in the demographic component of the simulation.

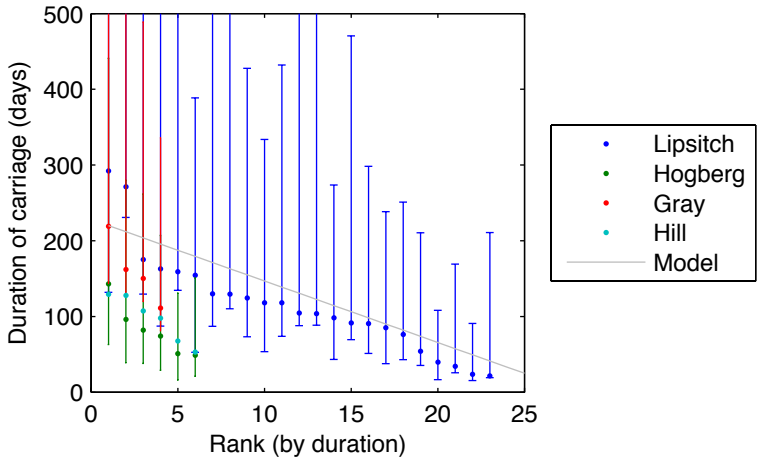

Fig. S6

Durations of carriage measured in Lipsitch et al. (*9*) in children <22 mos. old for individual serotypes, Högberg et al. (*8*) in children <1 y old for serotypes/serogroups, Gray et al. (*17*) in infants with primary, secondary, or tertiary colonization for serotypes/serogroups, and Hill et al. (*12*) in infants at primary colonization for serotypes. Error bars show ranges of observed durations for Högberg et al. and Gray et al. and credible intervals for Lipsitch et al. Only mean durations were reported by Hill et al. The durations used in the default model are shown by a gray line for comparison.

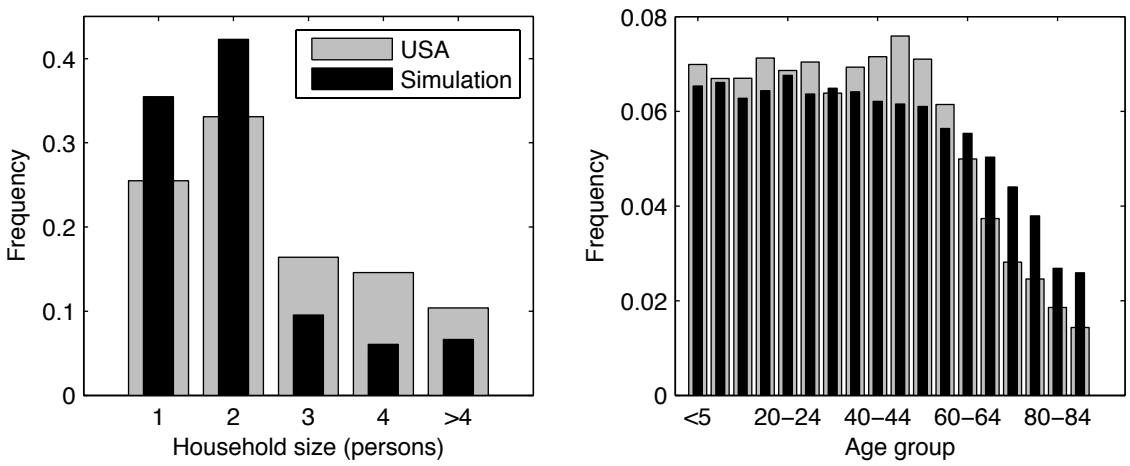

Fig. S7

Comparison of the final distributions of household sizes and ages from a sample simulation to the corresponding rates in the U.S. population in 2000 and 2008, respectively (*46*). The demographic dynamics were very similar across the simulations.

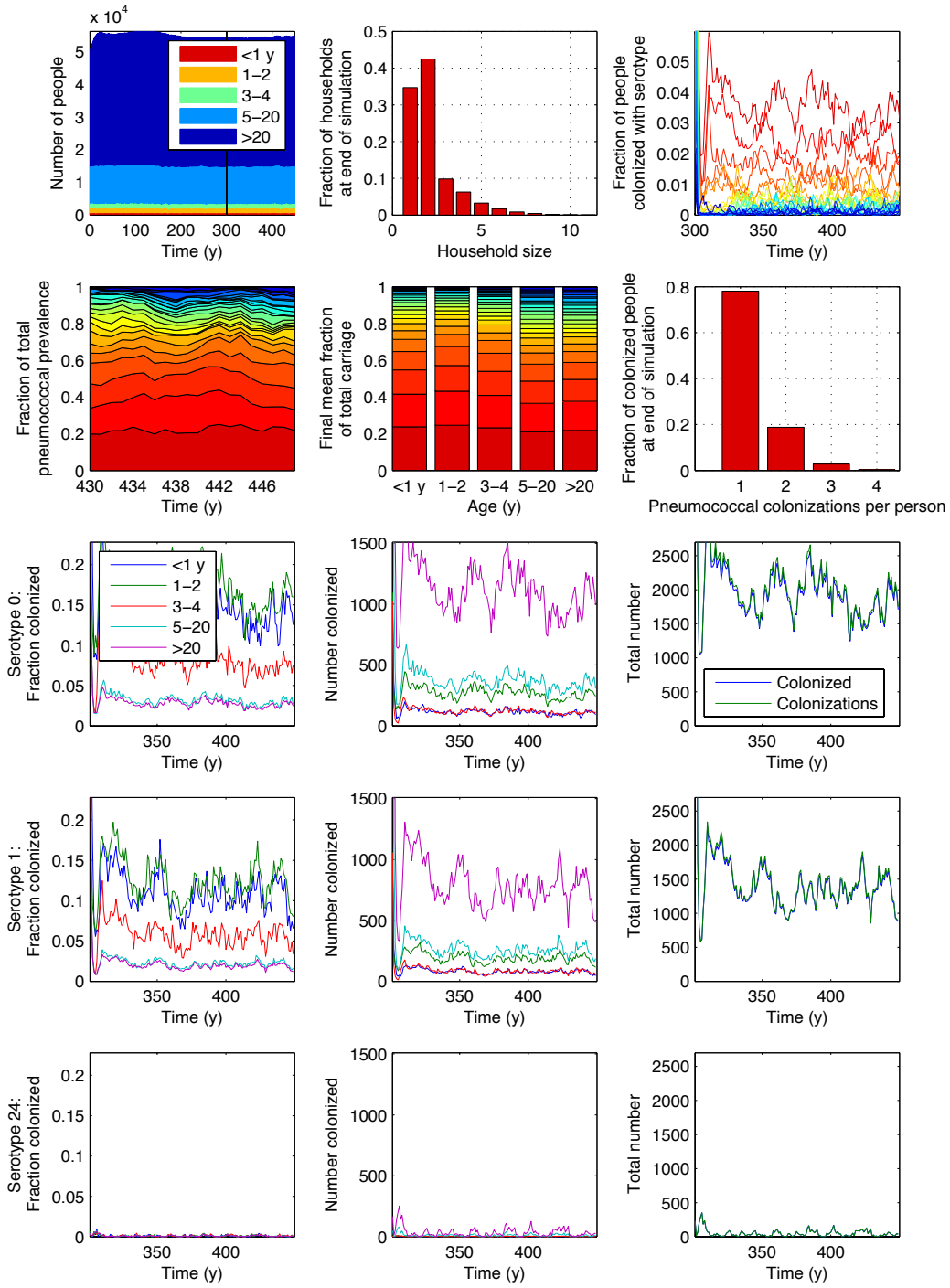

Fig. S8

Summary of one simulation ($\sigma = 0.3,\ \varepsilon = 0.25$). Where not otherwise indicated, colors indicate serotypes' fitnesses, with the most (least) fit serotype shown in red (blue). For brevity, detailed trajectories are shown only for the most fit ("Serotype 0"), second most fit ("1"), and least fit ("24") serotypes. "Colonized" refers to the number of people colonized with each serotype, and "colonizations" refers to the total number of strains of a serotype that are colonizing hosts.

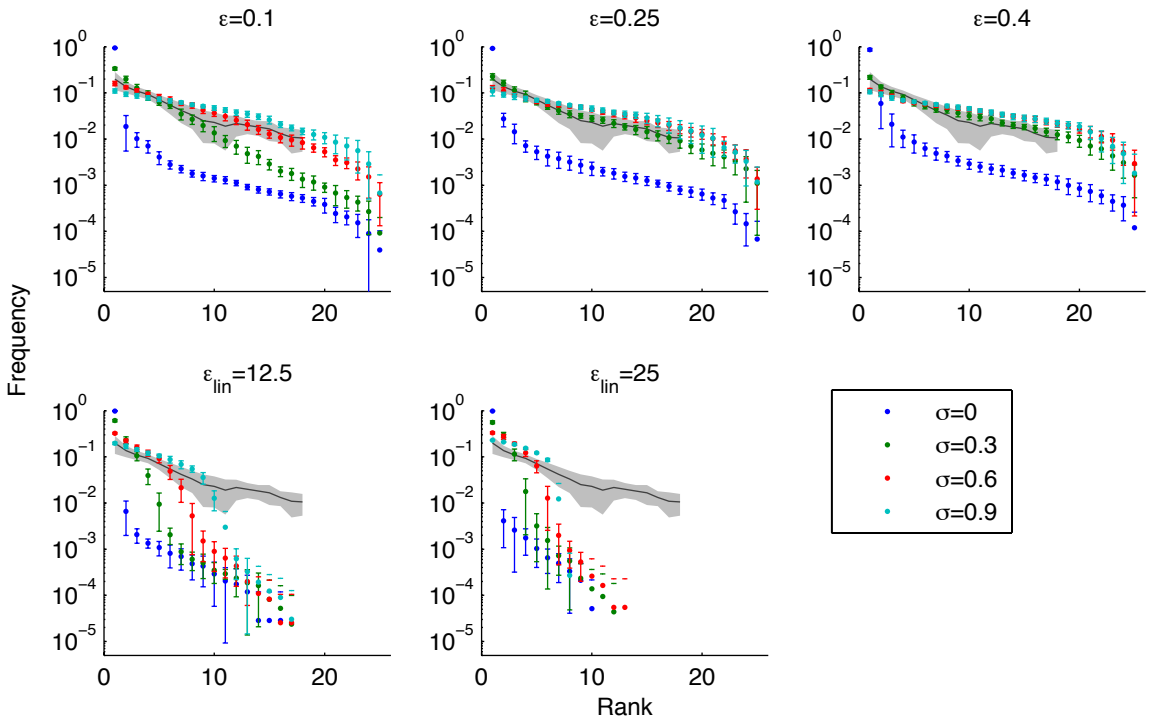

Fig. S9

Rank-frequency distributions produced by simulations with anticapsular immunity levels of $\sigma = 0$, 0.3, 0.6, and 0.9 for different models of nonspecific immunity. Error bars show standard deviations from ten simulations. The dark gray curve in each plot shows the mean rank-frequency distribution from carriage studies and the shading two standard deviations.

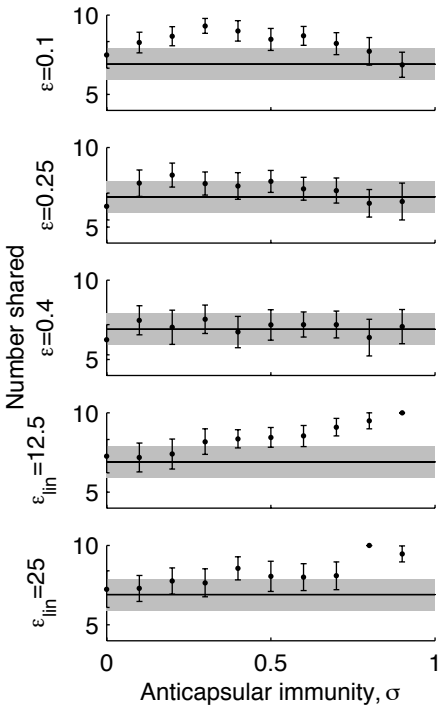

Fig. S10

The average number of serotypes in common out of the ten most frequent serotypes in replicate simulations of different models of immunity. Numbers were averaged across ten simulations; error bars show standard deviations. Serotype frequencies were measured in the final year of simulation. The simulation estimates are superimposed on the mean (black line) and standard deviation (gray area) of the number shared in carriage studies.

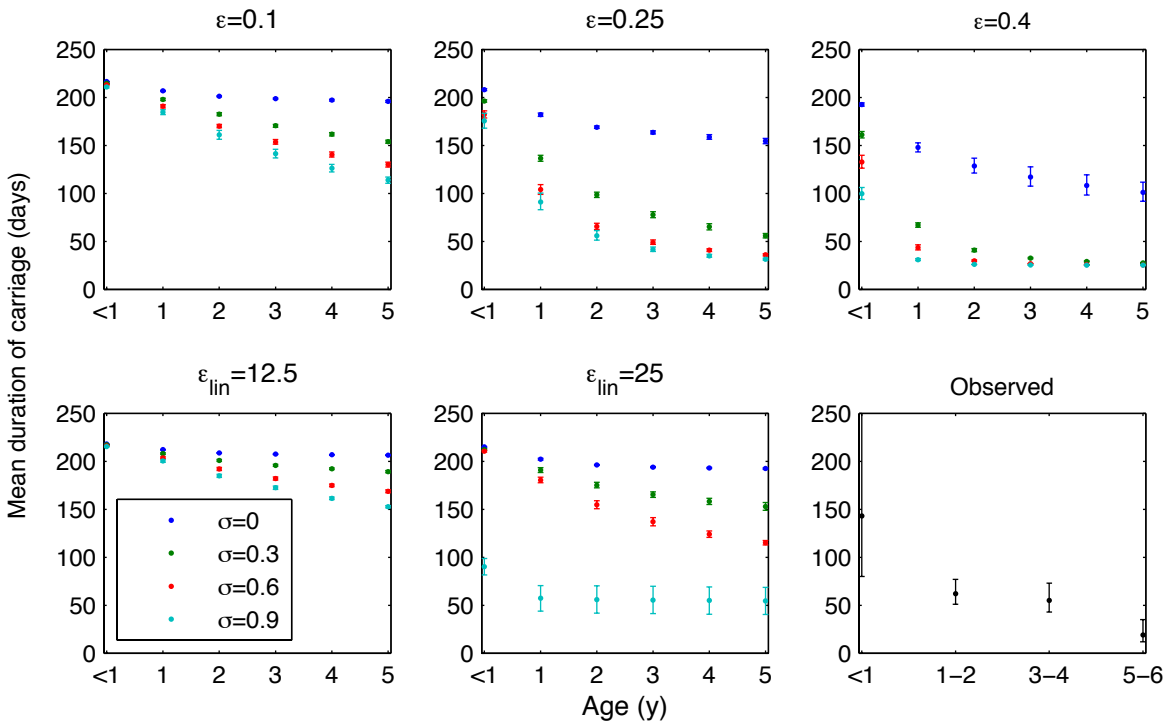

Fig. S11

Simulated and observed relationships between the mean duration of carriage (for the fittest serotype) and age. For simulations, results are shown for different strengths of anticapsular immunity ($\sigma = 0$, 0.3, 0.6, and 0.9). Error bars show standard deviations from the means of ten simulations. Observed durations of carriage are shown for serogroup 6, one the most common serogroups and the serogroup with the longest initial observed duration in (*8*). Error bars show the range observed in the study.

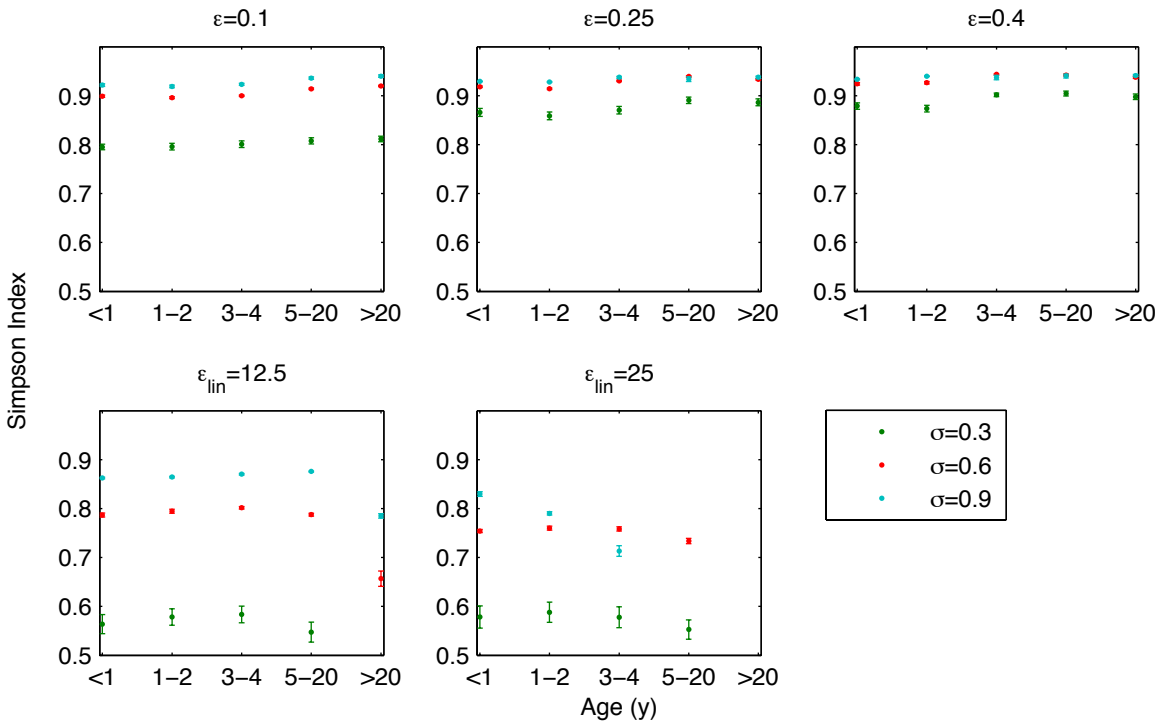

Fig. S12

The relationship between serotype diversity (measured by the Simpson Index), anticapsular immunity ($\sigma = 0.3$, 0.6, and 0.9), and host age. Values for $\sigma = 0$ are not shown because they maintained a constant value of ~0.2 and did not vary significantly with age. Error bars show standard deviations from the means of ten simulations.

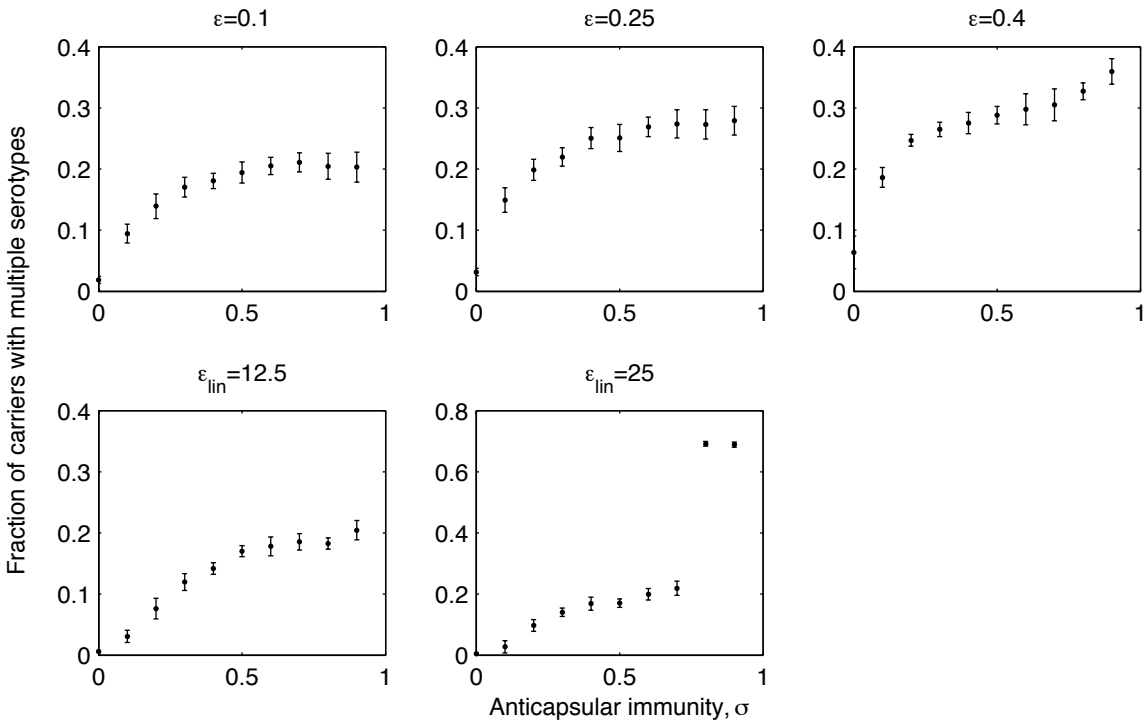

Fig. S13

The fraction of carriers <5 y old colonized with multiple serotypes at different levels of anticapsular immunity and immune models. Note that the subplot for $\varepsilon_{lin} = 25$ has different limits to its *y*-axis that the other plots. Error bars show standard deviations from ten simulations.

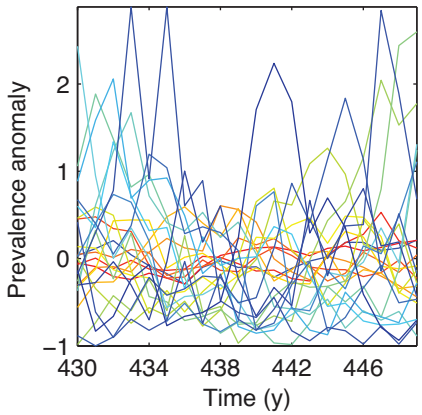

Fig. S14

Deviation of each serotype from its mean prevalence (normalized to zero) in the last 20 y of a sample simulation with $\sigma = 0.3$. The colors indicate serotypes' fitnesses, with the most (least) fit serotype shown in red (blue).

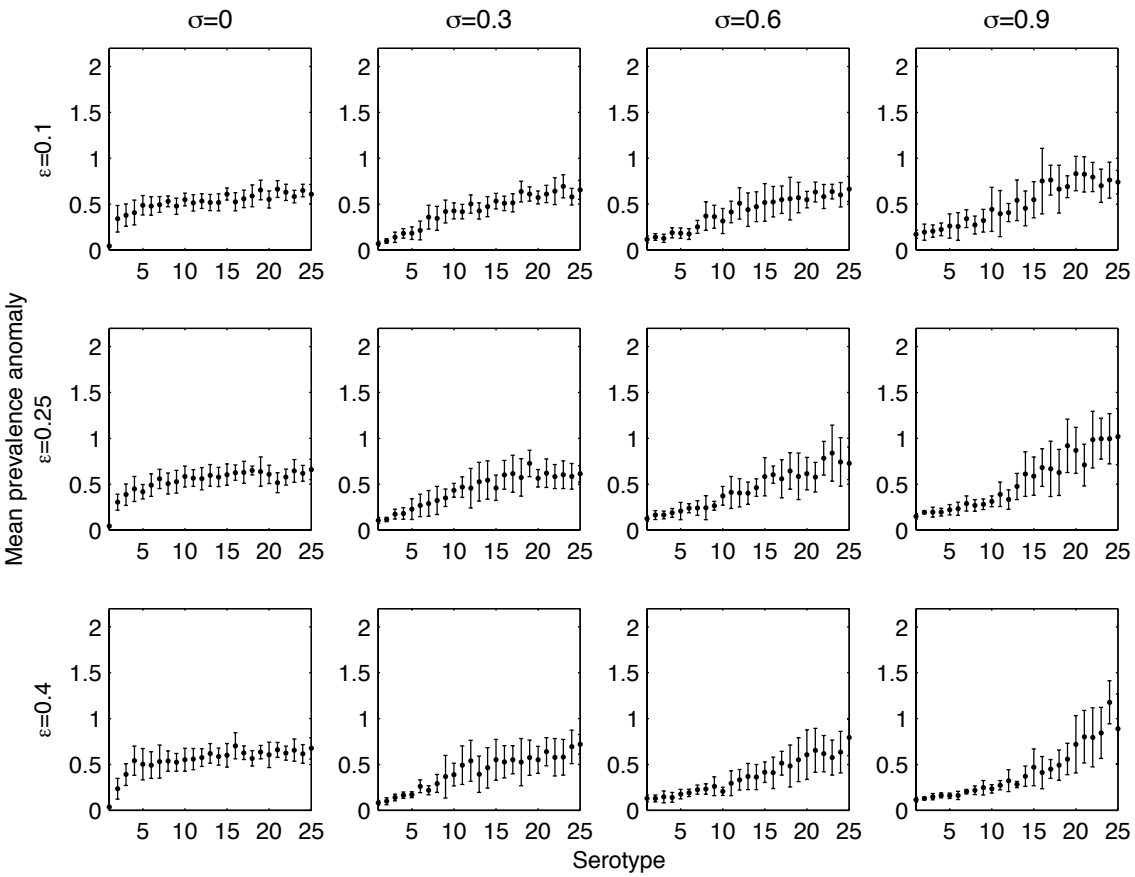

Fig. S15

The mean prevalence anomaly of each serotype, with the serotypes arranged in descending order of intrinsic fitness. Data were taken from the last 20 y of simulations. Error bars show standard deviations from ten simulations.

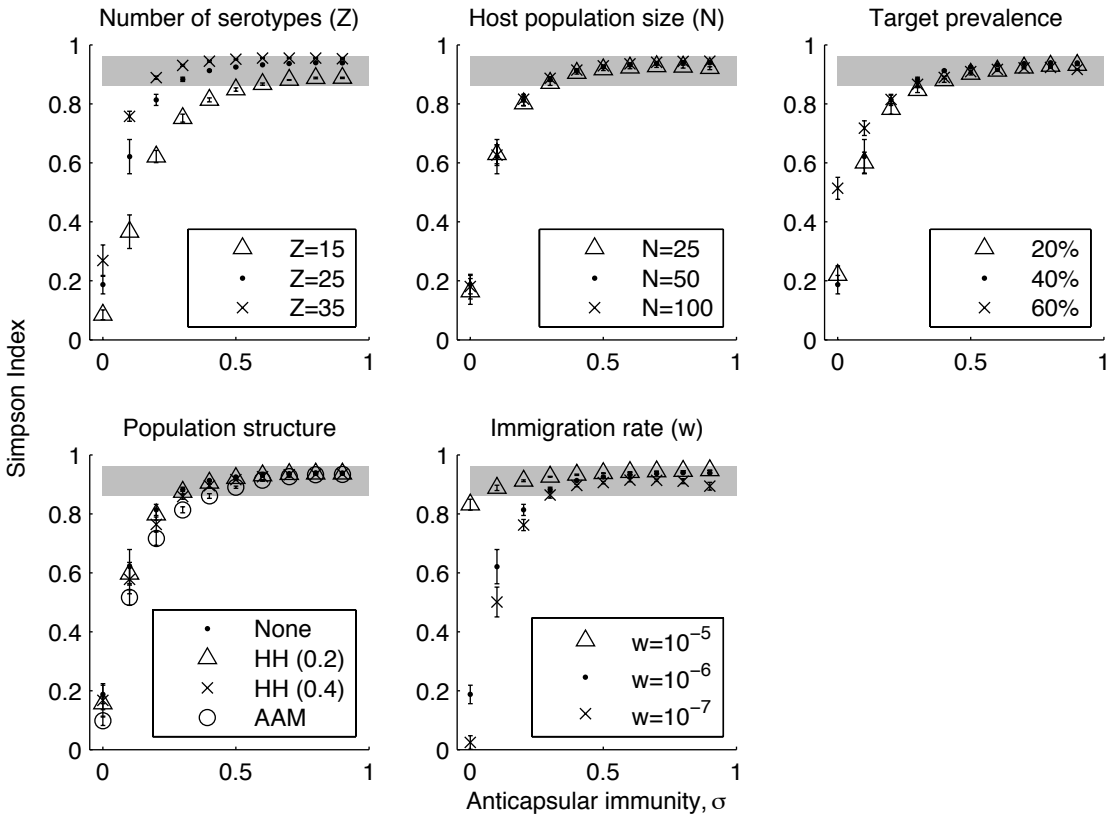

Fig. S16

Sensitivity analysis of pneumococcal diversity (as measured by the Simpson Index) under varying levels of anticapsular immunity. For models with $Z = 15$, 25, and 35 serotypes, in each model, the intrinsic durations of carriage were spaced evenly over the interval [25 days, 220 days]. Host population sizes are shown in thousands. In the subplot for host population structure, results from the default model with random mixing are given by "None", household structure ("HH") is shown for within-household contact probabilities $\rho = 0.2$ and $\rho = 0.4$, and age-assortative mixing is indicated by "AAM". Error bars show standard deviations from ten simulations.

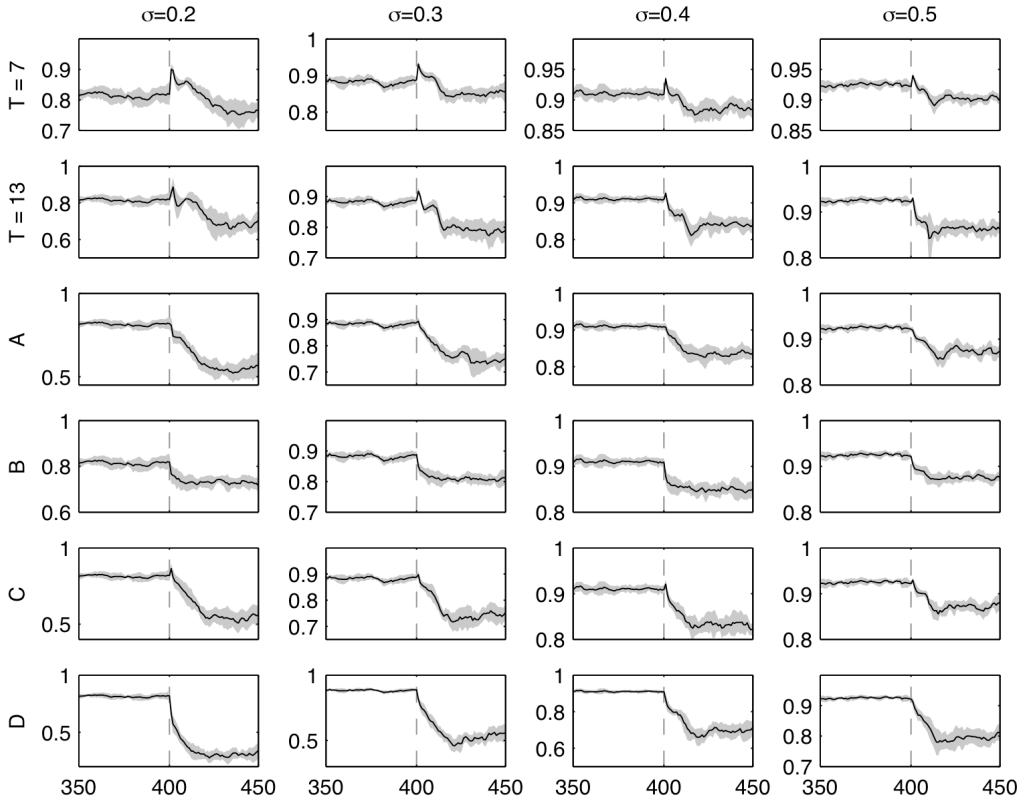

Fig. S17

Simpson Index in children <5 y old as a function of time (in y) for different vaccine scenarios and levels of anticapsular immunity σ. Gray areas show standard deviations from ten simulations.

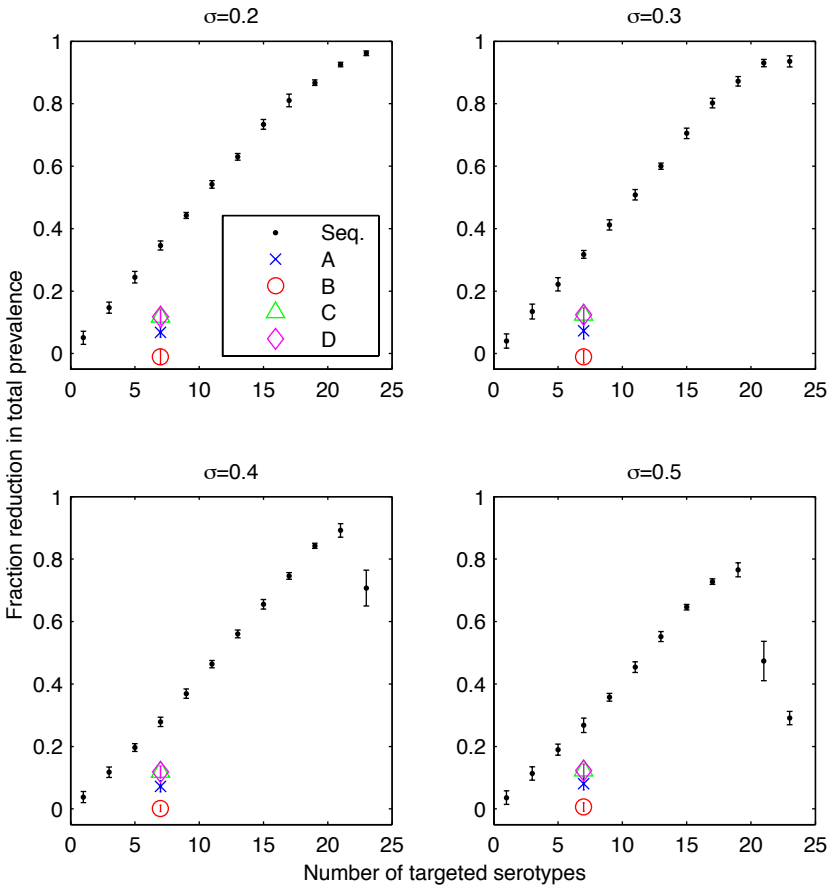

Fig. S18

Long-term reduction in total carriage prevalence in children <5 y old following vaccination as a fraction of pre-vaccine carriage prevalence. Pre-vaccine carriage prevalence was estimated as the ten-year average before vaccination and the post-vaccine carriage as the average in years 410-419. The "Seq." points refer to scenarios in which the T most fit serotypes were targeted, and A-D refer to scenarios in Table S3. Error bars show standard deviations from ten simulations. As the strength of natural anticapsular immunity approaches that of vaccine-induced immunity, vaccines that target the majority of serotypes ($T = 21$ and $T = 23$ for $\sigma = 0.5$) allow the resurgence of the most fit serotypes as soon as a decade following vaccination, causing total carriage prevalence to be higher than with lower-valent vaccines that allow natural immunity from nontargeted types to contribute to the suppression of targeted types.

Table S1.

Summary of studies included in carriage analysis; DCC = day-care center.

Study	Age range	No. of typed isolates	Percent reporting specific serotype	Simpson Index	Carriage prevalence (%) or percent of positive isolates
Infants					
Bogaert et al. 2001 (*47*)	3-36 mos	303	72	-	35* (unweighted mean of DCCs and non-DCCs)
Charveriat et al. 2005 (*48*)	2-24 mos	~473	68	-	52
Cheung et al. 2009 (*49*)	9-15 mos, younger sibs	1315	92	-	86
Dagan et al. 1996 (*50*)	10-22 mos	102	72	-	44
Darboe et al. 2010 (*51*)	5 mos	172	100	0.94	88
Givon-Lavi et al. 1999 (*52*)	12-35 mos	72	100	0.86	77* (mean for all DCCs)
Young children (including infants)					
Abdullahi et al. 2008 (*20*)	0-5 y	205	100	0.93	57
Espinosa de los Monteros et al. 2007 (*53*)	2 mos – 6 y	829	100	0.88	30
Factor et al. 2005 (*54*)	2-59 mos	224	61	-	59
Ho et al. 2004 (*55*)	2-6 y	353	75	-	19
Huang et al. 2005 (*56*)	0-7 y	190	82	-	26
Huebner et al. 2000 (*57*) **	1-60 mos	121	100	0.88	40
Katsarolis et al. 2009 (*58*)	Median age 4.3 ± 1.1 y	114	76	-	29
Kellner & Ford-Jones 1999 (*59*)	34 ± 17 mos, 91% <5 y	589	100	0.88	44
Marchisio et al. 2001 (*60*)	0-7 y	242	61	-	9
Mastro et al. 1993 (*61*)	2-59 mos	131	100	0.94	62
Millar et al. 2009 (*62*)	0-6 y	532	78	-	65
Nunes et al. 2005 (*63*)	6 mos – 6 y	178	89	-	63
Quintero et al. 2011 (*64*)	2-5 y	61	100	0.91	28
Regev-Yochay et al. 2004 (*65*)	3 wks – 6 y	200	56	-	53
Rivera-Olivero et al. 2007 (*66*)	0-72 mos	92	89	-	49* (mean of total)
Roche et al. 2007 (*67*)	6 mos – 5 y	120	86	-	51
Vestrheim et al. 2008 (*40*)	10-69 mos	485	100	0.92	78
Zemlickova et al. 2006 (*68*)	3-6 y	165	100	0.89	38
Older children and adults					
Abdullahi et al. 2008 (*20*)	≥5 y	72	100	0.96	14
Bokaeian et al. 2011 (*69*)	10-19 y	119	100	0.93	16
Mixed age groups					
Abdullahi et al. 2008 (*20*)	Random	277	100	0.94	31
Hill et al. 2008 (*12*)	Random	2369	70	-	72
Hussain et al. 2005 (*70*)	Families	901	79	-	25
Leino et al. 2008 (*71*)	Families, DCC workers	70	87	-	11* (mean of total)
		63	95	-	
		70	95	-	

*The carriage prevalence or mean number of positive isolates was not reported for the specific population listed in the table. The closest estimate is reported with a short description. **This study did not state the duration of its enrollment period, but it is implied to be short.

Table S2.

Default and alternate parameter values used in the models. PMF = probability mass function.

Symbol	Description	Default value	Alternate(s)	Refs.
Demographic parameters				
N(0)	Initial population size (in thousands)	50	25, 100	-
-	PMF of age at death	(Fig. S5)	-	(*72*)
-	PMF of maternal age at birth	(Fig. S5)	-	(*73*)
-	PMF of number of offspring in lifetime	(Fig. S5)	-	Calculated so no net growth
-	PMF of age of departing from family of origin	(Fig. S5)	-	Assumed similar to ages at partnering
-	PMF of age at initiating partnering	(Fig. S5)	-	(*46*)
-	Age range of acceptable partners relative to self	[-3,3] y	-	Mean age difference (*46*)
-	Fraction of the population that ever partners	0.9	-	(*46*)
Epidemiological parameters				
Z	Number of serotypes	25	15, 35	-
-	Initial fraction of the population colonized with each serotype *z*	0.02	-	-
β	Baseline rate of contact of each colonization with serotype *z*	Fitted to obtain 40% prevalence in kids <5 y	20%, 60%	Consistent with observed prevalences (Table S1)
$\gamma(z)$	Intrinsic duration of carriage of a strain of serotype *z*	25-220 days	-	(*8, 17*)
κ	Minimum duration of carriage of a strain of pneumococcus	25 days	-	(*8*)
w	Per capita rate of "immigration" of each serotype	10^{-6} host^{-1} day^{-1}	-	-
ε	Shape parameter for the reduction in duration of carriage dependent on past colonizations	0.25	ε = 0.1, 0.4 and ε_{lin} = 12.5, 25	Fitted by nonlinear least squares from (*17*)
σ	Reduction in susceptibility to a serotype conferred by prior carriage of that serotype	-	Varied over [0,0.9]	(*11*)
μ_{max}	Reduction in susceptibility to pneumococcus from carrying the fittest serotype	0.25	-	(*9*)
α	Age-associated weights on contact rates	Random mixing	α used	(*36, 74*)
ρ	Fraction of contacts within household	Random mixing	0.2, 0.4	(*75*)
…with vaccination				
p	Per-person vaccine efficacy	0.6	-	Estimated (*23*)
a_v	Age at receiving vaccine	6 months	-	Recommended is 2, 4, 6, 12-15 mos; incomplete dosing effective (*76*)

Table S3.

Fitness rankings of targeted serotypes (4, 6B, 9V, 14, 18C, 19F, and 23F) as inferred by serotypes' frequencies in carriage or durations of carriage. When the rank of serotype 4 was not given, it was assigned the rank following the maximum rank in the study. Scenario E was used as the example in the main text.

Source	Scenario	Age group	Ranks of targeted serotypes
Averages of studies in young children (Fig. S3)	A	Most <5 y (see Table S1)	1, 3, 4, 8, 12, 21, 25
Lipsitch et al. (*9*), based on Abdullahi et al. (*20*)	B	<22 mos.	4, 6, 8, 10, 17, 18, 24
Hussain et al. (*70*) (as reported in (*25*))	C	<5 y	1, 2, 4, 5, 9, 12, 21
	D	>20 y	2-7, 21
	E	All (families)	1-4, 8, 11, 21

SOM References

33. S. van Selm, L. M. van Cann, M. A. Kolkman, B. A. van der Zeijst, J. P. van Putten, *Infect Immun* **71**, 6192 (Nov, 2003).
34. E. Meats *et al*., *J Clin Microbiol* **41**, 386 (Jan, 2003).
35. E. H. Simpson, *Nature* **163**, 688 (1949).
36. J. Mossong *et al*., *PLoS Med* **5**, e74 (Mar 25, 2008).
37. D. Bogaert, D. Weinberger, C. Thompson, M. Lipsitch, R. Malley, *Infect Immun* **77**, 1613 (Apr, 2009).
38. S. D. Brugger, L. J. Hathaway, K. Muhlemann, *J Clin Microbiol* **47**, 1750 (Jun, 2009).
39. P. Turner *et al*., *J Clin Microbiol* **49**, 1784 (May, 2011).
40. D. F. Vestrheim, E. A. Hoiby, I. S. Aaberge, D. A. Caugant, *J Clin Microbiol* **46**, 2508 (Aug, 2008).
41. M. Gratten *et al*., *Southeast Asian J Trop Med Public Health* **20**, 501 (Dec, 1989).
42. Y. Sun, Y. Hwang, M. H. Nahm, *Infect Immun* **69**, 336 (Jan, 2001).
43. S. S. Huang *et al*., *Pediatrics* **124**, e1 (Jul, 2009).
44. J. Spijkerman *et al*., *Emerg Infect Dis* **17**, 584 (Apr, 2011).
45. R. Cohen *et al*., *Vaccine* **28**, 6114 (Aug 23, 2010).
46. K. Faust, in *The Methods and Materials of Demography,* J. Siegel, D. Swanson, Eds. (Elsevier Academic Press, Boston, 2004).
47. D. Bogaert *et al*., *J Clin Microbiol* **39**, 3316 (Sep, 2001).
48. M. A. Charveriat, M. Chomarat, M. Watson, B. Garin, *Med Mal Infect* **35**, 500 (Oct, 2005).
49. Y. B. Cheung *et al*., *Pediatr Infect Dis J* **28**, 990 (Nov, 2009).
50. R. Dagan *et al*., *J Infect Dis* **174**, 1271 (Dec, 1996).
51. M. K. Darboe, A. J. Fulford, O. Secka, A. M. Prentice, *BMC Infect Dis* **10**, 195 (2010).
52. N. Givon-Lavi, R. Dagan, D. Fraser, P. Yagupsky, N. Porat, *Clin Infect Dis* **29**, 1274 (Nov, 1999).
53. L. E. Espinosa-de Los Monteros *et al*., *Salud Publica Mex* **49**, 249 (Jul-Aug, 2007).
54. S. H. Factor *et al*., *Emerg Infect Dis* **11**, 1476 (Sep, 2005).
55. P. L. Ho *et al*., *Vaccine* **22**, 3334 (Sep 3, 2004).
56. S. S. Huang *et al*., *Pediatrics* **116**, e408 (Sep, 2005).
57. R. E. Huebner, A. D. Wasas, K. P. Klugman, *S Afr Med J* **90**, 1116 (Nov, 2000).
58. I. Katsarolis *et al*., *BMC Infect Dis* **9**, 120 (2009).
59. J. D. Kellner, E. L. Ford-Jones, *Arch Pediatr Adolesc Med* **153**, 495 (May, 1999).
60. M. Marchisio *et al*., *Am J Pathol* **159**, 803 (Sep, 2001).
61. T. D. Mastro *et al*., *Pediatr Infect Dis J* **12**, 824 (Oct, 1993).
62. E. V. Millar *et al*., *Pediatr Infect Dis J* **28**, 711 (Aug, 2009).
63. S. Nunes *et al*., *J Clin Microbiol* **43**, 1285 (Mar, 2005).
64. B. Quintero *et al*., *Eur J Clin Microbiol Infect Dis* **30**, 7 (Jan, 2011).
65. G. Regev-Yochay *et al*., *Clin Infect Dis* **38**, 632 (Mar 1, 2004).
66. I. A. Rivera-Olivero *et al*., *Clin Infect Dis* **45**, 1427 (Dec 1, 2007).
67. A. Roche *et al*., *Arch Dis Child* **92**, 1073 (Dec, 2007).

68. H. Zemlickova *et al*., *Epidemiol Infect* **134**, 1179 (Dec, 2006).
69. M. Bokaeian, H. Khazaei, M. Javadimehr, *Iranian Red Crescent Medical Journal* **13**, 328 (2011).
70. M. Hussain *et al*., *Epidemiol Infect* **133**, 891 (Oct, 2005).
71. T. Leino, F. Hoti, R. Syrjanen, A. Tanskanen, K. Auranen, *BMC Infect Dis* **8**, 173 (2008).
72. H. J. Kintner, in *The Methods and Materials of Demography,* J. S. Siegel, D. A. Swanson, Eds. (Elsevier Academic Press, Boston, 2004), pp. 303-304.
73. S. Estee, in *The Methods and Materials of Demography,* J. S. Siegel, D. A. Swanton, Eds. (Elsevier Academic Press, San Diego, CA, 2004).
74. Unknown, in *Vital Statistics: Population and Health Reference Tables*. (Office for National Statistics, 2011).
75. F. Hoti, P. Erasto, T. Leino, K. Auranen, *BMC Infect Dis* **9**, 102 (2009).
76. E. J. van Gils *et al*., *JAMA* **302**, 159 (Jul 8, 2009).